RESEARCH ARTICLE

Macromolecular Chemistry and Physics
www.mcp-journal.de

Multimodal Polymeric Crosslinker Capable of Dual Crosslinking for Enhanced Cohesion, Adhesion, and Debonding of Waterborne Acrylic Adhesives

*Seoyoon Yu and Chaenyung Cha**

Waterborne acrylic adhesives, despite their widespread usage, often suffer from insufficient cohesive and adhesive properties, especially compared to solvent adhesives. Therefore, in order to improve the performance of waterborne adhesives, it is important to enhance and control these properties in a refined manner. For this purpose, herein presents a polymeric crosslinker presenting a variable number of methacrylic groups intended to control the degree of crosslinking. Polysuccinimide (PSI), which consists of a series of succinimidyl rings, is conveniently modified with methacrylic functional groups by ring-opening nucleophilic reaction to develop methacrylic PSI ("MA-PSI"). The cohesion and adhesion of MA-PSI crosslinked adhesive is comprehensively controlled by both concentration and degree of methacrylic substitution (DS_{MA}) of MA-PSI. Moreover, the dual crosslinking, accomplished by the successive application of thermal- and photo-crosslinking, further increases the cohesion to the extent that significantly reduces the adhesion strength, which is ideal for debonding applications. Overall, the multimodal MA-PSI is a versatile crosslinker allowing broad controllability of cohesion and adhesion as well as imparting debonding capability.

1. Introduction

Waterborne adhesives have gained significant attention in recent years, due to the rising concern over the toxic nature of more conventional solvent-based adhesives that contain volatile organic compounds (VOC).[1–4] The waterborne adhesives generally utilize aqueous-dispersible polymers in water as a solvent, and thermally cured by evaporating water without using toxic VOC's. In addition to environmental friendliness and safety, they are also easy to handle and mold, since they exist mostly in emulsions having high viscosity. As a result, they are also widely used as inks for printing, painting, and thin film coating.[5]

Despite the wide applicability of waterborne adhesives, they still suffer from lower mechanical strength, durability, and adhesive strength, especially compared to solvent-based adhesives, which must be substantially improved for better performance.[6,7] Since the water is the medium, the polymerization reactions are less efficient, and the types of monomers, macromers, and catalysts that can be used under aqueous environment are limited. On the other hand, the solvent-based adhesives do not have those same restrictions, hence the chemical reactions are much more efficient.

Crosslinking has been commonly applied to improve the cohesion and adhesion of waterborne adhesives for its efficiency, since the crosslinking reaction can proceed concurrently during the curing process.[7–11] Increased cohesion can prevent premature structural disintegration upon external force, thereby enhancing the adhesion and prolonging the lifetime. There have been a number of crosslinkers developed thus far, but the common feature is having two or more reactive functional groups that can link different polymer chains, such as ethylene glycol di(meth)acrylate and its oligomeric and polymeric versions (e.g., poly(ethylene glycol) di(meth)acrylate (PEGD(M)A)) for acrylic adhesives.[12,13]

While the conventional crosslinkers have been shown to be effective, their properties and functions still need further improvement for better controllability. For instance, most small molecular crosslinkers have limited aqueous solubility, since the reactive functional groups are mostly hydrophobic. As a result, the amount of crosslinkers that can be included in the aqueous resin becomes restricted, limiting the range of crosslinking density. Polymeric crosslinkers with higher aqueous solubility such as PEGDMA may be used, but the number of reactive functional groups per molecule is not significant enough to induce more expansive polymeric network.

Interestingly, lower cohesive and adhesive strengths of waterborne adhesives have in fact become an advantage in certain applications that require debonding.[2,14–16] Often referred to as temporary bonding and debonding ("TBDB"), the TBDB

S. Yu, C. Cha
Department of Materials Science and Engineering
Center for Multidimensional Programmable Matter
Ulsan National Institute of Science and Technology (UNIST)
Ulsan 44919, Republic of Korea
E-mail: ccha@unist.ac.kr
S. Yu
Center for Specialty Chemicals
Korea Research Institute of Chemical Technology (KRICT)
Ulsan 44412, Republic of Korea

The ORCID identification number(s) for the author(s) of this article can be found under https://doi.org/10.1002/macp.202400415

DOI: 10.1002/macp.202400415

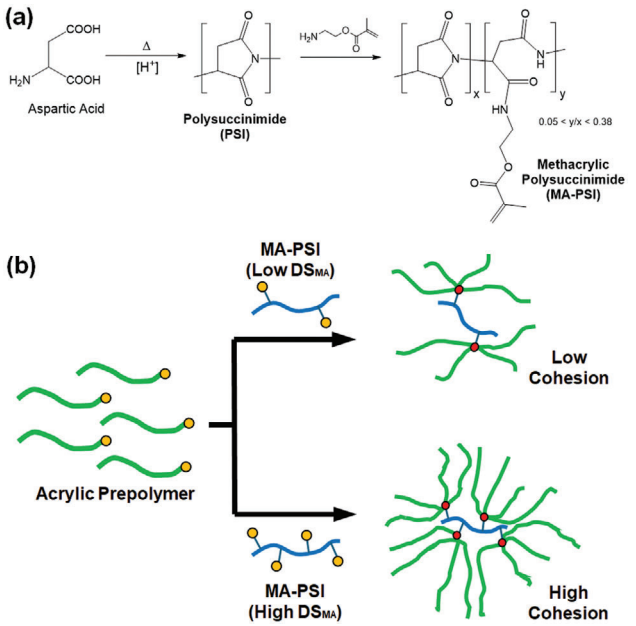

Figure 1. (a) Synthesis of methacrylic polysuccinimide (MA-PSI). (b) Schematic illustration of crosslinking acrylic prepolymer with MA-PSI with different degrees of methacrylic substitution (DS_{MA}) to control the cohesion.

adhesives have become a commonplace in many packaging applications as pressure-sensitive adhesives, from simple paper notes and box glues to more sophisticated semiconductor packaging process.[17] Most debonding is accomplished by simply applying physical force, often at elevated temperature to reduce the adhesive strength.[18] More recently, research efforts are underway to develop "on-demand" debonding technology, in which the debonding process is initiated, or "triggered", by external stimuli, such as light and electromagnetic field.[19–21]

In this study, a multimodal polymeric crosslinker capable of controlling the crosslinking density of waterborne acrylic adhesive was developed. Polysuccinimide (PSI), consisting of a series of succinimidyl ring moieties, can accommodate various functional groups by ring-opening nucleophilic reaction with amine-based molecules.[22–24] To allow the crosslinking reaction by radical copolymerization, methacrylic groups were conjugated to PSI backbone, termed MA-PSI, by ring-opening nucleophilic addition with 2-aminoethyl methacrylate (AEMA) (**Figure 1**). The degree of methacrylate substitution of MA-PSI was conveniently controlled by the feed molar ratio. In order to assess the effect of MA-PSI crosslinking on the cohesive and adhesive properties of waterborne acrylic adhesives, the mechanical and rheological properties of MA-PSI-crosslinked adhesives were assessed, while lap-shear tests were performed to evaluate the adhesive properties. Furthermore, the ability of MA-PSI to induce debonding was evaluated by applying dual-crosslinking, i.e., thermal- and photo-crosslinking reactions in sequence, to induce more extensive crosslinking reaction, which was expected to reduce the adhesion by excessive increase in cohesion.[8]

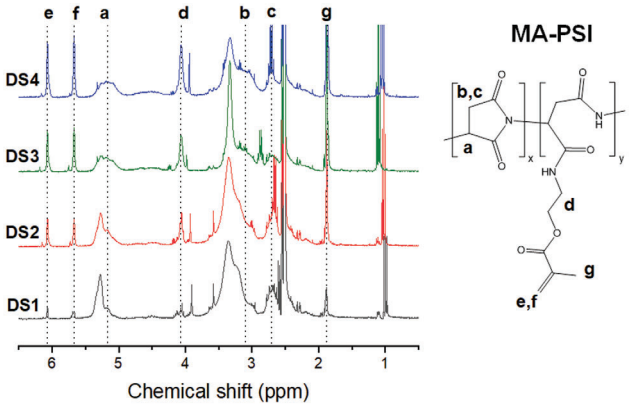

Figure 2. ^{1}H-NMR spectra of MA-PSI with various DS_{MA}'s from DS1 to DS4. Characteristic peaks associated with MA-PSI are denoted (a–g).

2. Results and Discussion

2.1. Synthesis and Characterization of MA-PSI

MA-PSI was conveniently synthesized by direct ring-opening nucleophilic addition between PSI and AEMA under ambient conditions without a catalyst (Figure 1a). The feed molar ratio of AEMA to PSI was varied to control the degree of methacrylate substitution of MA-PSI (DS_{MA}). MA-PSI's with four different DS_{MA}'s were successfully synthesized. ^{1}H-NMR spectra clearly showed the presence and increasing intensities of methacrylic peaks (**Figure 2**). The molecular weight, as determined from gel permeation chromatography (GPC), also increased accordingly with DS_{MA} due to the increasing amount of conjugated methacrylic groups (Table S1, Supporting Information). The four DS_{MA}'s calculated from the characteristic peak integration of NMR spectra, denoted as DS1-DS4, were 5, 15, 30, and 38%, demonstrating the controllability of methacrylate conjugation (Table S2, Supporting Information), illustrating the efficiency of nucleophilic reaction with PSI that allowed a wide range of methacrylate conjugation.

2.2. Cohesive and Adhesive Properties of MA-PSI-Crosslinked Adhesives

2.2.1. Effect of DS_{MA} and Concentration of MA-PSI

The lap-shear test was performed to measure shear modulus and adhesive strength in order to determine the effect of concentration and DS_{MA} of MA-PSI on the adhesive properties of the waterborne acrylic adhesives (**Figure 3a**; Figure S3, Supporting Information). The waterborne acrylic resin including MA-PSI was thermally crosslinked, during which methacrylate on PSI was expected to participate in the radical polymerization with the acrylic prepolymers. In addition, it was further hypothesized that the unreacted succinimidyl groups could also possibly react with carboxylic acid groups on AA units and hydroxyl groups on HEMA units of the acrylic prepolymer, further providing the crosslinking.[25] At the lowest DS_{MA} (DS1), increasing concentra-

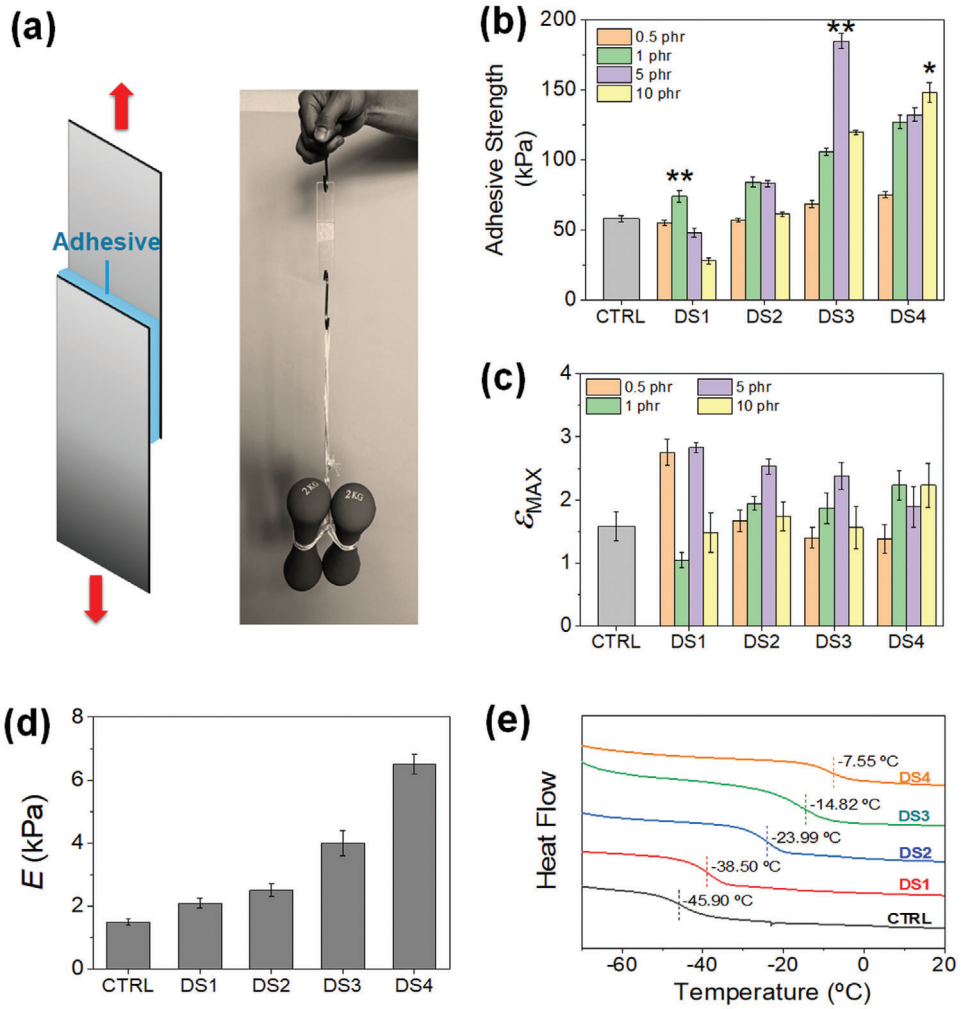

Figure 3. (a) Schematic illustration of a lap-shear test and demonstration of adhesive strength by hanging a heavy object (4 kg). (b) Adhesive strength and (c) maximum strain (ϵ_{max}) values of MA-PSI-crosslinked acrylic adhesives obtained from the lap-shear test. The concentration and DS_{MA} of MA-PSI were varied ($^{*}p < 0.05$, $^{**}p < 0.01$ compared at the same DS_{MA}, $n = 6$). (d) Elastic moduli (E) and (e) differential scanning calorimetric curves of MA-PSI-crosslinked acrylic adhesives with varying DS_{MA} (at 5 phr). The glass transition temperatures (T_g) are identified. The acrylic adhesive cured without the crosslinker was used as a control (CTRL).

tion of MA-PSI did not result in any significant change in adhesive strength up to 1 phr. Further increase in concentration rather reduced the adhesive strength (Figure 3b). This result suggested that the number of methacrylic groups on PSI for DS1 was too low to participate in the crosslinking reaction, and the increasing presence of MA-PSI rather prevented self-crosslinking of acrylic prepolymers.

At higher DS_{MA}, there was more pronounced increase in adhesive strength with increasing MA-PSI concentration. With increasing DS_{MA} from DS1 to DS3, the adhesive strength gradually increased at a given concentration. For example, the adhesive strength increased from 43 to 185 kPa when increasing DS_{MA} from DS1 to DS3 at 5 phr of MA-PSI. This observation strongly suggested that the increasing presence of methacrylic groups on MA-PSI was sufficient enough to undergo crosslinking reaction with the acrylic prepolymers, enhancing the adhesion. The degree of increase in adhesive strength increased with concentration up to 5 phr, as expected, but there was a significant reduction at 10 phr, even though the adhesive strength did increase with DS_{MA}. This meant that the concurrent decrease in acrylic prepolymer content relative to MA-PSI was too much to be compensated by increased level of crosslinking of MA-PSI.

It is interesting to note that the adhesion strength did not continue to increase with further increase in DS_{MA} up to DS4 at 5 phr. Rather, there was a significant reduction in adhesive strength at 5 phr when DS_{MA} was increased from DS3 to DS4 (Figure 3b). This could be attributed to the increased hydrophobicity of MA-PSI with DS_{MA}, caused by the hydrophobic nature of methacrylic groups.[26,27] Therefore, at the highest DS_{MA}, the crosslinking reaction between MA-PSI and the acrylic prepolymer could not efficiently proceed due to the lowered miscibility between MA-PSI and the acrylic prepolymer. Another possibility was the excessive increase in cohesion caused by the increased crosslinking causing the adhesion strength to decrease. Excessive increase in cohesion has been well known to decrease in adhesion, as more adhesive polymers being crosslinked interact more with each

other, rather than forming adhesive interaction with the material surface.[8,28]

The maximum strain (ϵ_{max}), at which the maximum adhesion strength occurred, represented the ability to maintain the structural integrity and adhesion while undergoing deformation (Figure 3c). Generally, the trend of ϵ_{max} with MA-PSI concentration was opposite to that of adhesion strength at the lowest DS_{MA} (DS1), having higher adhesion strength at lower ϵ_{max}, due to more acrylic polymers interacting with MA-PSI rather than the surface, resulting in detachment at lower strain. However, at higher DS_{MA} of DS3 and DS4, ϵ_{max} increased with MA-PSI concentration and followed the same trend of adhesion strength. This signified that higher degree of chemical crosslinking by the increased presence of methacrylate could more effectively hold the acrylic polymers, while allowing adhesive physical interaction with the surface, thereby resisting the structural failure even at higher strain conditions.

To explore the possibility of excessive increase in cohesion with increasing DS_{MA} causing adhesion to diminish at 5 phr, the mechanical rigidity of the MA-PSI-crosslinked adhesives was evaluated by measuring the elastic modulus via uniaxial compression (Figure 3d). The modulus continued to increase with DS_{MA} even at DS4, which proved the continued increase in crosslinking density. The glass transition temperature (T_g), as determined from differential scanning calorimetry (DSC), also increased with DS_{MA} of MA-PSI (Figure 3e). Therefore, this result strongly suggested that the decrease in adhesive strength at DS4 was likely caused by the excessive increase in cohesion preventing adhesive interaction at the interface.

At the highest MA-PSI concentration of 10 phr, the adhesive strength gradually increased up to DS4, from 32 to 143 kPa, as a result of the substantial increase in the number of methacrylic groups that could crosslink more acrylic prepolymers despite the rise in hydrophobicity. Still, it was lower than that of DS3 at 5 phr, 185 kPa, which further highlighted the importance of finding the balance between providing a sufficient number of reactive functional groups for crosslinking and the miscibility between the acrylic prepolymer and the crosslinker that could maximize the physical interaction with the waterborne acrylic prepolymers.

The adhesive shear modulus was also determined along with the adhesive strength from the lap shear test (Figure S4, Supporting Information). Regardless of the concentration and DS_{MA} of MA-PSI, the trend of shear moduli exactly followed that of adhesive strength. This result signified that the cohesion imparted by the crosslinking of MA-PSI-crosslinked was the driving force of the overall adhesive strength, since the shear modulus largely represents the cohesive strength of the adhesive measured under small deformation, while the adhesive strength represents the contribution from the interfacial adhesive bonds as well as cohesive strength resisting large deformation. This is not surprising, given that the chemical composition of the adhesives was not significantly changed, all consisting of acrylic prepolymers and MA-PSI.

The fact that the adhesive strength remained low for MA-PSI at lower DS_{MA}, regardless of concentration, which has more unreacted succinimidyl groups that could theoretically undergo ring-opening reaction with hydroxyl and carboxylic groups of acrylic prepolymers. This meant that the possibility of crosslinking reaction via ring-opening reaction of PSI was either nonexistent or not a contributing factor in the crosslinking process.

2.2.2. Dual Crosslinking: Thermal- and Photo-Crosslinking

Even though thermal-crosslinking was shown to be effective in inducing the crosslinking reaction, resulting in concurrent increase the adhesion strength, it was speculated that further crosslinking could be possible, since the heat treatment often leads to continuous solvent (water) evaporation, during which the reaction rate diminishes accordingly by the limited mobility of acrylic prepolymers. Also, the acrylic emulsion does not contain a large amount of free acrylic groups, as most of the monomers have reacted to become polymers. As a result, some of the prepolymers and MA-PSI were expected to remain unreacted under the given temperature. Therefore, it was hypothesized that applying additional crosslinking could further increase cohesion, which in turn could modulate the adhesion.

To examine the possibility of dual-crosslinking capability of MA-PSI-based acrylic adhesive, thermal- and photo-crosslinking steps were performed in sequence (**Figure 4a**; Figures S5 and S6, Supporting Information). The order of crosslinking was varied; thermal-crosslinking followed by photo-crosslinking ("T_C-UV_C") or photo-crosslinking followed by thermal-crosslinking ("UV_C-T_C"). Their cohesive and adhesive properties were compared with those made only with thermal-crosslinking ("T_C") shown in Figure 3. For T_C-UV_C, the initial heat treatment resulted in the gradual loss of the solvent (water) via evaporation, which could potentially hamper efficient photo-crosslinking due to the limited mobility of polymers lowering the reactivity. Nevertheless, the unreacted prepolymers and MA-PSI present in an enriched environment were expected to be sufficient enough to allow UV-initiated photo-crosslinking reaction. In order to confirm the dual-crosslinking reactions, the gel fraction and elastic moduli were measured. The gel fraction, which accounts for the fully-crosslinked, non-dissolvable portion of the adhesive, clearly showed that both T_C-UV_C and UV_C-T_C contained substantially larger amounts of crosslinked portion than T_C, which proved the dual-crosslinking method was indeed effective in further promoting the degree of crosslinking (Figure 4b). Expectedly, the elastic moduli of T_C-UV_C and UV_C-T_C were both substantially higher than those of T_C (Figure 4c). Furthermore, the degree of increase from T_C also was the largest at the highest DS_{MA} for both T_C-UV_C and UV_C-T_C, suggesting that the remaining MA-PSI with higher DS_{MA} could more extensively participate in the subsequent crosslinking reaction.[29,30] It is also noteworthy that the elastic moduli of the dual-crosslinked adhesives were unaffected by the order of crosslinking, regardless of DS_{MA} of MA-PSI, indicating that the initial crosslinking could proceed to a certain extent under the given reaction condition, leaving a significant portion of prepolymer and MA-PSI unreacted, and the additional crosslinking process involving a different mode of initiation could react the remaining ones to completion.

The change in ϵ_{max} with DS_{MA} for UV_C-T_C showed a notable dependence on MA-PSI concentration (Figure S7, Supporting Information). At lower concentration (1 phr), ϵ_{max} increased with DS_{MA}, while the opposite trend was shown at higher concentration (5 phr), even though the adhesive strengths generally in-

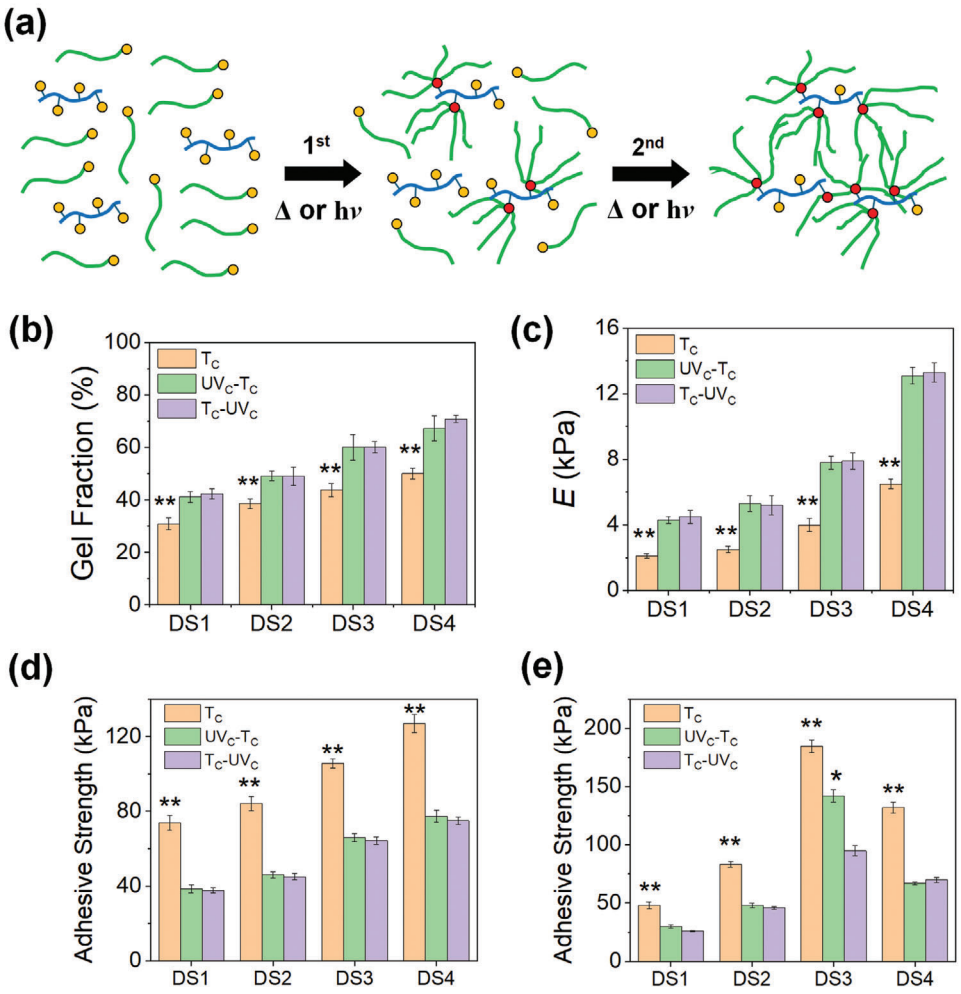

Figure 4. (a) Schematic illustration of dual-crosslinking of MA-PSI, applying thermal- (T_C) and photo-crosslinking (UV_C) in sequence, to maximize the degree of crosslinking. The order was changed; UV_C followed by T_C (UV_C-T_C), or T_C followed by UV_C (T_C-UV_C). (b) Gel fraction and (c) elastic moduli (E) of the MA-PSI-crosslinked adhesives at 5 phr. Adhesive strengths obtained by lap-shear test: (d) 1 phr and (e) 5 phr (*$p < 0.05$, **$p < 0.01$ compared at the same DS_{MA}, $n = 6$).

creased with DS_{MA} for both concentrations. It was speculated that there was an insufficient amount of methacrylic groups at lower concentration in that a greater amount of methacrylic groups at higher DS_{MA} was needed to sufficiently induce photo-crosslinking to resist externally applied force, while the degree of photo-crosslinking was sufficiently high enough at higher concentration that excessive increase in cohesion likely resisted mechanical deformation and yielded at lower strain at higher DS_{MA}. In comparison, ϵ_{max} was less affected by the DS_{MA} for T_C-UV_C. The initial thermal treatment possibly helped the adhesive polymers regardless of DS_{MA} anneal more evenly to the surface.

The adhesive properties of dual-crosslinked adhesives were examined by measuring the shear modulus and adhesive strength in order to assess the effect of enhanced cohesion on the adhesive properties. The most notable observation was the decrease in shear modulus and adhesive strength for both T_C-UV_C and UV_C-T_C regardless of DS_{MA} and concentration of MA-PSI (Figure 4d,e; Figure S8, Supporting Information). This result, similar to the lowered adhesive strength for the highest DS_{MA} at 5 phr, was a clear indication that the extent of enhanced cohesion by the dual crosslinking was too critical that it prevented adhesive polymers from strong adhesive interaction with the surface. At higher concentration of 5 phr, the adhesive strength was higher for UV_C-T_C than T_C-UV_C, especially at higher DS_{MA} of MA-PSI. Since the initial photo-crosslinking during UV_C-T_C did not result in the solvent evaporation, the adhesive polymers could still more freely interact with the material surface, while the initial thermal-crosslinking for T_C-UV_C likely made the adhesive more cohesive. Another possibility is the loss of interfacial peel strength by the breakdown of adhesive bonds between the adhesive and the material surface by the high intensity of UV irradiation.[31,32] In any case, the adhesive strengths by both T_C-UV_C and UV_C-T_C decreased almost by half at the highest DS_{MA}. Unlike 5 phr, the difference in adhesive strength between UV_C-T_C and T_C-UV_C and among different DS_{MA}'s was negligible at 1 phr. Since there was lesser amount of unreacted MA-PSI remaining after initial crosslinking, the additional crosslinking possibly consumed most of MA-PSI regardless of DS_{MA}.

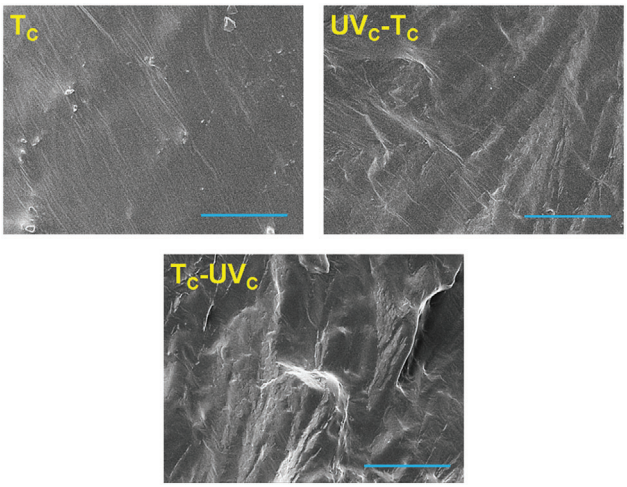

Figure 5. SEM images of MA-PSI-crosslinked acrylic adhesives prepared by dual-crosslinking (UV_C-T_C, UV_C-T_C) and single crosslinking (T_C) (scale bar: 100 μm).

This critical loss of adhesion strength for the dual-crosslinked adhesives could be viewed as having ideal properties for TBDB applications. The debonding of most conventional TBDB adhesives often involves a harsh thermomechanical process, where adhesive and cohesive strengths of the adhesive are first reduced by heat treatment, usually above the glass transition temperature and enough for at least the partial decomposition, followed by the mechanical force. Recent research efforts have been geared toward developing "debonding-on-demand" adhesive that can be more easily debonded by an external trigger such as light, electrical, and chemical treatment.[19–21] Since the additional crosslinking, either thermal or photo-crosslinking, resulted in a significant loss of adhesive strength that allows easier debonding, the MA-PSI-crosslinked adhesive could be utilized for versatile TBDB applications. While previous debonding-on-demand approaches often involve different chemical routes and additional chemicals for crosslinking and debonding, the debonding of MA-PSI is conveniently imparted by dual crosslinking for thermomechanical or photomechanical debonding.

SEM was used to visualize the morphological features of the MA-PSI-crosslinked adhesives to further evaluate the different modes of crosslinking (**Figure 5**). It was immediately evident that T_C demonstrated smoother texture, while dual-crosslinked adhesives showed more extensive wrinkles. This increased surface roughness was another indication of the higher degree of crosslinking of dual-crosslinked adhesives. Between T_C-UV_C and UV_C-T_C, T_C-UV_C showed higher surface roughness, having deeper grooves with more wrinkles, which partly explained their difference in adhesive strength. Despite having similar mechanical rigidity, the adhesive strength was lower for T_C-UV_C at a given DS_{MA} and concentration of MA-PSI. The additional photo-crosslinking more greatly altered surface texture, having rougher surface, making it more susceptible for detachment. While heat treatment could more homogeneously affect the adhesive structure, UV irradiation has a greater effect on the surface than the interior, as the UV intensity diminishes with penetration depth. Consequently, there was a greater degree of photo-crosslinking on the surface, leading to more pronounced surface roughness.

In order to further highlight the degree of control of adhesive properties by MA-PSI with both DS_{MA} and concentration, two commercially-available, aqueous-soluble crosslinkers, triethylene glycol dimethacrylate (TEGDMA) and PEGDMA were used to crosslink the acrylic adhesives as control groups (Figure S9, Supporting Information). They both consist of hydrophilic ethylene glycol repeating units and methacrylic end groups, only differ in their molecular weights; 286 Da for TEGDMA and 550 Da for PEGDMA. Thus, at the same concentration, the number of methacrylic groups would be higher for TEGDMA, thus leading to higher crosslinking density. As expected, the adhesive shear modulus and adhesive strength were higher for TEGDMA-crosslinked adhesives than PEGDMA-crosslinked adhesives. However, they showed much more limited ranges than MA-PSI-crosslinked adhesives under the same range of concentrations, from 0.5 to 10 phr, including both T_C and dual crosslinking (UV_C-T_C and T_C-UV_C). The adhesive strength ranged from 130 to 210 kPa for TEGDMA-crosslinked adhesives and 105 to 190 kPa for PEGDMA-crosslinked adhesives. This is obviously due to the fact that unlike MA-PSI, it is not possible for TEGDMA and PEGDMA to control the number of methacrylic groups per chain. This result further highlighted the critical advantage of MA-PSI as a multivalent crosslinker for waterborne acrylic adhesives.

2.3. Rheological Properties of MA-PSI-Crosslinked Adhesive

The rheological properties of the MA-PSI-crosslinked adhesive were evaluated by measuring the changes in storage (G') and loss (G'') moduli over time from the onset of crosslinking via rotational rheometry (**Figure 6a–d**). The rate of crosslinking was first evaluated by measuring the gel time, the time for the increasing G' to cross over the G'' (Figure 6e).[33] At the lowest DS_{MA} (DS1), the gel time increased with MA-PSI concentration, which correlated with the decreasing adhesive strength shown in Figure 3, another indication that the crosslinking between MA-PSI and acrylic prepolymers could not proceed efficiently having lower number of methacrylate. On the other hand, the gel time decreased with MA-PSI concentration at higher DS_{MA}, clearly indicating the elevated rate of crosslinking by the increased amount of methacrylate participating in the reaction.

The maximal G' values measured after crosslinking also reflected the increased cohesion and adhesion by the crosslinking with MA-PSI. The G' values became much higher with MA-PSI concentration at a given DS_{MA}, especially at higher DS_{MA}, which was similarly demonstrated for the adhesive properties. Tangent delta (tan δ), defined as the ratio of G'' to G' that represents the relative proportions of viscous and elastic contents, can determine the relative contribution of physical association and chemical crosslinking on the cohesive and adhesive properties (**Figure 7**). While the mechanical rigidity and adhesive strength increased accordingly with the DS_{MA} and concentration of MA-PSI, tan δ did not show any significant change with concentration up to DS3, which meant that there was still a significant portion of physical association between the acrylic prepolymer and MA-PSI in addition to the chemical crosslinking. At the highest

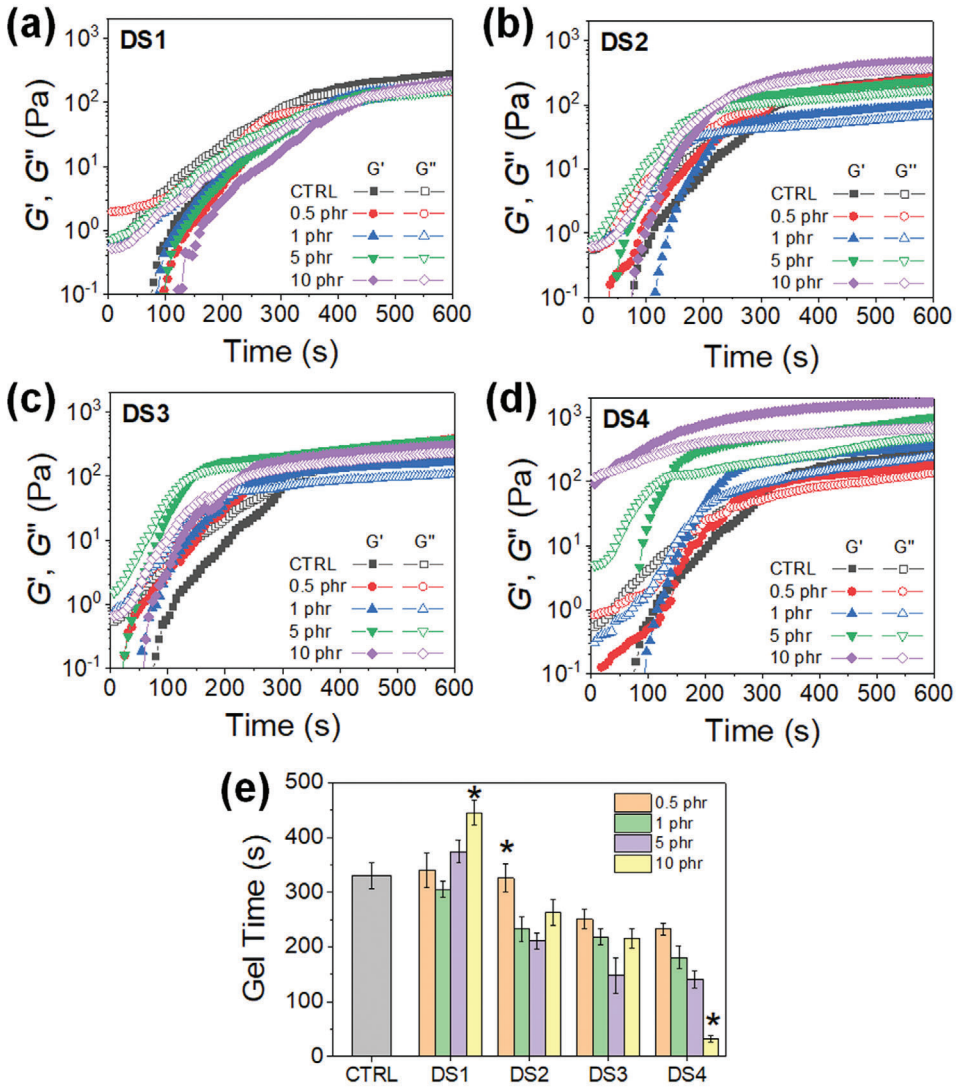

Figure 6. Storage (*G'*) and loss (*G"*) moduli of MA-PSI-crosslinked acrylic adhesives with varying concentrations and DS_{MA}'s of MA-PSI obtained from rotational rheometry: (a) DS1, (b) DS2, (c) DS3, and (d) DS4. (e) Gel times of MA-PSI-crosslinked acrylic adhesives, determined as the time for the increasing *G'* to cross over *G"* as shown in (a–d) (*$p < 0.05$, compared at the same DS_{MA}, $n = 6$).

DS_{MA} of DS4, however, tan δ decreased substantially with MA-PSI concentration, clearly suggesting that the critical increase in the number of methacrylic groups on PSI could more effectively link the adhesive prepolymers. Taken all together, MA-PSI was demonstrated to be a versatile polymeric crosslinker capable of refined control of cohesion and adhesion of waterborne acrylic adhesives.

3. Conclusion

In this study, the polysuccinimide (PSI) functionalized with tunable number of methacrylic groups, termed MA-PSI, was developed as a multifunctional polymeric crosslinker to control the cohesion and adhesion of waterborne acrylic adhesives. The degree of methacrylic substitution (DS_{MA}) could be conveniently controlled by varying the feed molar ratio of the reactant, AEMA, to PSI, as AEMA can directly react with PSI via ring-opening nucleophilic addition without any additives. By measuring the adhesive strength via lap-shear test and the mechanical rigidity via uniaxial compression, the resulting MA-PSI with variable DS_{MA} was shown to be highly effective in enhancing the cohesion and adhesion of the acrylic adhesive by providing more sites for crosslinking reaction. Moreover, applying consecutive crosslinking schemes with two different modes of initiation, thermal- and photo-crosslinking, could further increase the cohesive properties of the adhesive, as the initial crosslinking only proceeding to a certain extent leaves some of acrylic prepolymer and MA-PSI unreacted, which could then be more effectively reacted by providing a different initiation mechanism. The resulting dual-crosslinked adhesive was shown to display substantially decreased adhesive strength, caused by the excessive increase in cohesion. This interesting property of dual-crosslinkable MA-PSI could be potentially utilized as TBDB adhesives capable of "debonding-on-demand", Taken all together, MA-PSI is a highly

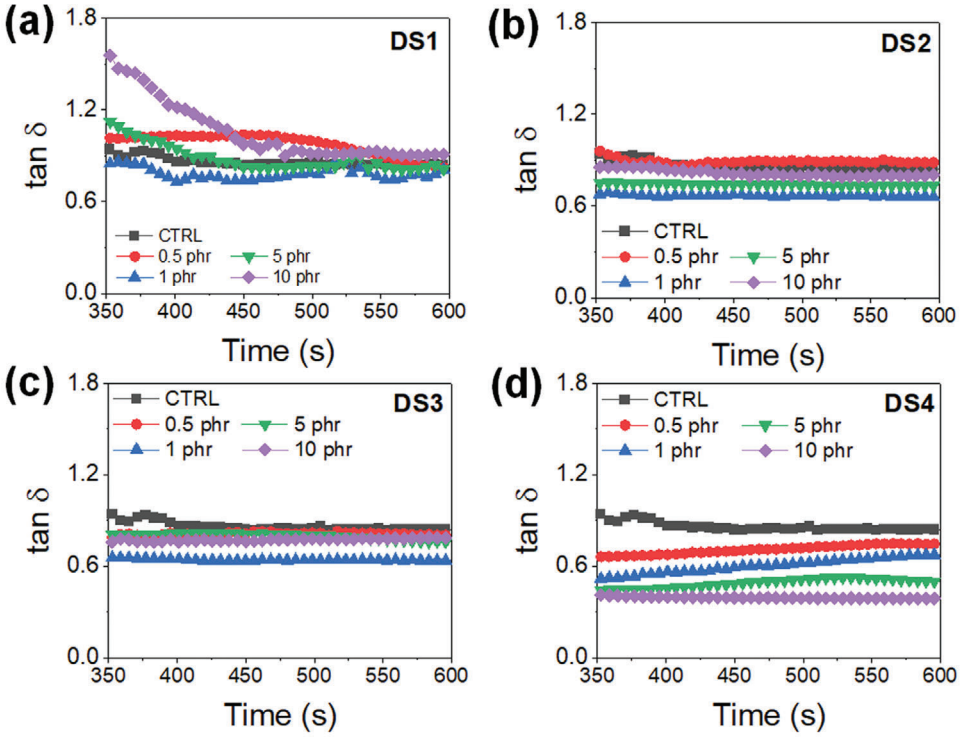

Figure 7. Tangent delta (tan δ), defined as the ratio of G'' to G', of MA-PSI-crosslinked acrylic adhesives with varying concentrations and DS_{MA}'s of MA-PSI, obtained from G' and G'' values presented in Figure 6: (a) DS1, (b) DS2, (c) DS3, and (d) DS4.

versatile crosslinker for waterborne acrylic adhesives, allowing not only enhanced cohesive and adhesive properties by varying the concentration and DS_{MA}, but also dual-crosslinking via two different modes of initiation to render the adhesive more susceptible for debonding.

4. Experimental Section

Materials: Ethanolamine hydrochloride, methacryloyl chloride, tetrahydrofuran (THF), hydroquinone, dimethyl sulfoxide (DMSO), triethylamine (TEA), *o*-phosphoric acid, *n*-butyl acrylate (n-BA), sodium dodecyl sulfate (SDS), and ammonium persulfate (APS) were obtained from Sigma–Aldrich (St. Louis, MO, USA). Methanol, L-aspartic acid, 2-ethyl hexyl acrylate (EHA), acrylic acid (AA), 2-hydroxyethyl methacrylate (HEMA), sodium carbonate (Na_2CO_3), and ethyl acetate (EtAc) were obtained from Samchun Chemicals Co. (Seoul, South Korea). Methyl methacrylate (MMA), sodium hydrogen carbonate ($NaHCO_3$), and sulfolane were purchased from Junsei Chemical Co. (Tokyo, Japan). Isopropyl alcohol (IPA) and *n*-pentane were purchased from Daejung Chemical Co. (Siheung, South Korea). All the chemicals were used without further purification.

Synthesis of Waterborne Acrylic Adhesive Resin: The waterborne acrylic adhesive resin was synthesized by a seeded semi-batch emulsion polymerization.[10,34,35] This process was used to generate an emulsion having a high number of highely-disperse, still-growing chains, rather than longer chains reached or close to termination with reduced dispersity, in order to be further processed by additional crosslinking process with MA-PSI.[36,37] For a typical experiment, 18.50 mL deionized (DI) water, 2.00 g SDS, and 53.30 g of total monomers were mixed with rigorous stirring to prepare a pre-emulsion solution. The monomers consisted of 65% EHA, 20% n-BA, 10% MMA, 3% AA, and 2% HEMA by weight. The buffer solution consisting of 0.33 g Na_2CO_3, 0.084 g $NaHCO_3$ in 18.5 mL DI water and the initiator solution consisting of APS as the radical initiator (0.33 g) in 1 mL DI water were separately prepared. 10% (v/v) of the total pre-emulsion and the APS solution were added to the buffer solution placed into a 250 mL three-neck flask equipped with a reflux condenser and a mechanical stirrer. The reaction mixture was stirred for 30 min under N_2 atmosphere at 80 °C to generate a high number of initial emulsion "seeds." Afterward, the rest of pre-emulsion was added to the mixture and further stirred for only for 2 h at 80 °C in order to retain a significant portion of chains under propagating state. The reaction mixture was cooled down to room temperature and quenched under ice, resulting in a stable and highly-dispersed emulsion which was used as the stock resin to be further crosslinked by MA-PSI for waterborne acrylic adhesive (Figure S10a, Supporting Information).

Synthesis of MA-PSI: PSI was obtained by acid-catalyzed polycondensation of aspartic acid.[22,23,38–40] First, 50 g L-aspartic acid and 1.22 mL *o*-phosphoric acid were added to 130 mL sulfolane and placed into a 250 mL three-neck flask equipped with a Dean-Stark trap and nitrogen inlet. The mixture was stirred at 180 °C for 7 h. The water produced during the reaction was continuously removed via a Dean-Stark trap. After the reaction, the red-orange solution was precipitated in excess methanol, and the precipitated product was collected by filtration. The crude product was washed several times with DI water until the pH became neutral. The final product was dried in vacuo. ^{1}H NMR (Bruker Advance 300 MHz, DMSO-d_6): δ (ppm) = 5.50–5.00 (1H, *m*), 3.20–2.90 (1H, *m*), 2.80–2.50 (1H, *m*) (Figure S1, Supporting Information).

The number-average molecular weight (M_n), weight-average molecular weight (M_w), and polydispersity index of PSI were determined by GPC (1260 series, Agilent Technologies, New York, NY, USA) equipped with two detectors; a refractometer and a viscometer. Each sample was dissolved in DMF at 0.1% (w/w) and filtered through a 0.2 µm membrane filter before loading into the column. The temperature was kept constant at 80 °C on both detectors and column. DMF was used as the eluent with a flow

rate of 1.0 mL min^{-1}. The molecular weight of the sample was calculated using the universal calibration technique with polyethylene oxide/glycol standards.

MA-PSI was synthesized by reacting PSI with varying amounts of AEMA. The detailed synthesis of AEMA is described in Figure S2 (Supporting Information). Briefly, PSI (2 g, 20 mmol) and TEA were first dissolved in 5 mL of DMSO, and then AEMA was added to the solution and stirred at room temperature for 72 h. The molar ratios of AEMA to succinimidyl groups of PSI were 5:100, 20:100, 50:100, and 80:100. The byproduct, TEA-HCl salt, generated during the reaction was eliminated by filtration. The product was obtained by precipitation in excess IPA and dried in vacuo. ^{1}H NMR (Bruker Advance 300 MHz, DMSO-d_6): δ (ppm) = 6.06 (1H, *s*), 5.66 (1H, *s*), 5.39–5.02 (1H, *m*), 4.13–3.99 (2H, *m*), 3.20–2.94 (1H, *m*), 2.83–2.58 (1H, *m*), 1.92–1.81 (3H, *m*). The degree of substitution of methacrylate on PSI was calculated by the integration ratio of methacrylic and PSI peaks.

Adhesive Curing: The adhesive resin was first prepared by mixing the acrylic resin stock, MA-PSI, and the photoinitiator (Irgacure2959). The concentrations of MA-PSI were 0.5, 1, 5, 10 parts per hundred resins (phr) of the acrylic resin stock, while the concentration of Irgacure2959 was fixed at 0.01 phr. The mixture was continuously stirred for 30 min until MA-PSI and Irgacure2959, and the resulting mixture retained the high dispersion of emulsion (Figure S10b, Supporting Information). For thermal-crosslinking, the resin was heated at 120 °C for 3 h. For photo-crosslinking, the resin was irradiated with UV (UVP Crosslinker CL-3000, Analytik Jena, 2000 mJ cm^{-2}) for 10 min to initiate the polymerization. For dual-crosslinking, the thermal-crosslinking and photo-crosslinking were performed successively.

Mechanical Characterization: The mechanical properties of the adhesive were evaluated by measuring the elastic modulus from uniaxial compression testing using a universal testing machine (Model 3343, Instron).[41–43] The adhesive was cured in between two glass plate with a 1 mm spacer, and cut into circular disks with 8 mm in diameter. The sample was compressed at the rate of 1 mm min^{-1}. The experiment was carried out at room temperature. The elastic modulus was calculated as the slope of the strain-stress curve at the initial linear region (10% strain). To assess the crosslinking density, gel fraction (W_g) was obtained by the following equation,

$$W_g = \frac{W_r}{W_i} \times 100 \quad (1)$$

where W_i was the initial weight of the sample and W_r was the residual weight of the sample.[44] Each sample was placed in toluene at 30 °C, and the residual part was collected by filtration and weighed after drying.

DSC (Q2000, TA Instruments) was performed on the crosslinked adhesive at a heating rate of 10 °C per min between −70 and 20 °C. After the first heating cycle, the second heating run was used to determine the glass transition temperature (T_g).

Field emission electron microscopy (FE-SEM) was used to visualize the detailed morphology of the adhesive (MIRA 3, Texcan). The surface of cured adhesive was sputter-coated with Pt and imaged under high vacuum mode.

Adhesive Characterization: Lap-shear tests were performed to measure the adhesive strength.[10,34] 0.1 g of the resin was placed between the overlapping area (25 × 25 mm) of two glass substrates, and cross-linked. The substrates were slowly pulled at the rate of 12 mm min^{-1}, and the stress-strain curve was obtained (Model 3343, Instron). The adhesive shear modulus was calculated the slope of the stress–strain curve at the initial linear region (10% strain), and the adhesive strength was chosen as the highest stress recorded during the experiment.

Rheological Characterization: The rheological characterizations of adhesives were performed using a rotating-disk rheometer (Discovery HR 20, TA instruments).[10,33,34] Storage and loss moduli were measured over time in a small-amplitude oscillatory shear mode with the strain of 10% and frequency of 1 Hz at 40 °C. The time it took for the storage modulus to cross over the loss modulus was chosen as the gelation time.

Statistical Analysis: Mean and standard deviation values from six independent experiments were reported in this study. The statistical significance of differences between the two conditions was assessed using Student's *t*-test. The statistical significance of the difference between multiple conditions was evaluated by one-way ANOVA followed by Tukey's post hoc test. *p*-values of 0.05 and below were considered statistically significant and are reported here.

Supporting Information

Supporting Information is available from the Wiley Online Library or from the author.

Acknowledgements

This study was supported by the Technology Innovation Program (or Industrial Strategic Technology Development Program) (20009198, Development and demonstration of biodegradable bioplastic prototype) funded by the Ministry of Trade, Industry & Energy (MOTIE, Korea) and Mid-Career Researcher Program through the National Research Foundation of Korea (NRF) funded by the Ministry of Science and ICT (2022R1A2C2009174)

Conflict of Interest

The authors declare no conflict of interest.

Data Availability Statement

The data that support the findings of this study are available from the corresponding author upon reasonable request.

Keywords

adhesion, cohesion, dual crosslinking, polysuccinimide, waterborne acrylic adhesives

Received: November 4, 2024
Revised: January 23, 2025
Published online:

[1] A. Santamaria-Echart, I. Fernandes, F. Barreiro, M. A. Corcuera, A. Eceiza, *Polymers* **2021**, *13*, 409.
[2] R. Jovanović, M. A. Dubé, *J. Macromol. Sci. C* **2004**, *44*, 1.
[3] Y.-K. Yang, H. Li, F. Wang, *J. Adhes. Sci. Technol.* **2003**, *17*, 1741.
[4] S. Yu, C. Cha, *Macromol. Res.* **2023**, *31*, 427.
[5] S. H. Imam, C. Bilbao-Sainz, B.-S. Chiou, G. M. Glenn, W. J. Orts, *J. Adhes. Sci. Technol.* **2013**, *27*, 1972.
[6] A. Agirre, J. Nase, E. Degrandi, C. Creton, J. M. Asua, *J. Polym. Sci., Part A: Polym. Chem.* **2010**, *48*, 5030.
[7] J. Kajtna, J. Golob, M. Krajnc, *Int. J. Adhes. Adhes.* **2009**, *29*, 186.
[8] Z. Czech, *Polym. Int.* **2003**, *52*, 347.
[9] J.-Y. Che, J.-M. Cheon, J.-H. Chun, C.-C. Park, Y.-H. Lee, H.-D. Kim, *J. Adhes. Sci. Technol.* **2017**, *31*, 1872.
[10] J. Hong, Y. Kwon, M. S. Kwon, C. Cha, *ACS Appl. Polym. Mater.* **2022**, *4*, 2105.
[11] H. Wahdat, M. Gerst, M. Rückel, S. Möbius, J. Adams, *Macromolecules* **2019**, *52*, 271.
[12] W. Gao, C. Li, J. Li, Q. Zhang, N. Wang, B. Abdel-Magid, X. Qu, *J. Adhes. Sci. Technol.* **2019**, *33*, 2031.

[13] G. Ceylan, S. Emik, T. Yalcinyuva, E. Sunbuloğlu, E. Bozdag, F. Unalan, *Polymers* **2023**, *15*, 2387.
[14] I. Márquez, N. Paredes, F. Alarcia, J. I. Velasco, *Polymers* **2021**, *13*, 2627.
[15] S. Mapari, S. Mestry, S. T. Mhaske, *Polym. Bull.* **2021**, *78*, 4075.
[16] M. Kim, Y. J. Jang, Y. Lee, C. Mun, H. Cho, H. Yoo, J. Koo, *Macromol. Res.* **2024**.
[17] Z. Mo, F. Wang, J. Li, Q. Liu, G. Zhang, W. Li, C. Yang, R. Sun, *Electronics* **2023**, *12*, 1666.
[18] K. R. Mulcahy, A. F. R. Kilpatrick, G. D. J. Harper, A. Walton, A. P. Abbott, *Green Chem.* **2022**, *24*, 36.
[19] M. Inada, T. Horii, T. Fujie, T. Nakanishi, T. Asahi, K. Saito, *Mater. Adv.* **2023**, *4*, 1289.
[20] C. Bandl, W. Kern, S. Schlögl, *Int. J. Adhes. Adhes.* **2020**, *99*, 102585.
[21] Z. Liu, F. Yan, *Adv. Sci.* **2022**, *9*, 2200264.
[22] J. Jang, C. Cha, *Biomacromolecules* **2018**, *19*, 691.
[23] M. Kim, C. Cha, *Biomacromolecules* **2020**, *21*, 3693.
[24] M. Kim, C. Choi, J. P. Lee, J. Kim, C. Cha, *Small* **2022**, *18*, 2107316.
[25] E. Jalalvandi, A. Shavandi, *Eur. Polym. J.* **2018**, *109*, 43.
[26] H. J. Zhang, X. Wang, Y. Yang, T. L. Sun, A. Zhang, X. You, *Macromolecules* **2022**, *55*, 7401.
[27] J. Hong, Y. Shin, S. Kim, J. Lee, C. Cha, *Adv. Funct. Mater.* **2019**, *29*, 1808750.
[28] Y. Yuan, X. Zhu, L. Chen, *Mater. Des.* **2020**, *185*, 108272.
[29] C.-M. Ryu, B.-L. Pang, J.-H. Han, H.-I. Kim, *J. Photopolym. Sci. Technol.* **2012**, *25*, 705.
[30] T. Ozawa, S. Ishiwata, Y. Kano, T. Kasemura, *J. Adhes.* **2000**, *72*, 1.
[31] H.-S. Joo, H.-S. Do, Y.-J. Park, H.-J. Kim, *J. Adhes. Sci. Technol.* **2006**, *20*, 1573.
[32] H.-H. Chu, C.-K. Wang, K. S. Chuang, C.-Y. Chang, *J. Polym. Res.* **2014**, *21*, 472.
[33] M. Kim, C. Cha, *Polymer* **2018**, *145*, 272.
[34] J. Han, J. Hong, C. Choi, C. Cha, *ACS Appl. Polym. Mater.* **2024**, *6*, 11167.
[35] L. Qie, M. A. Dubé, *Int. J. Adhes. Adhes.* **2010**, *30*, 654.
[36] C. Liu, A. K. Tripathi, W. Gao, J. G. Tsavalas, *Polymers* **2021**, *13*, 596.
[37] J. Khanjani, G. H. Zohuri, M. Gholami, B. Shojaei, R. Dalir, *J. Adhes.* **2014**, *90*, 174.
[38] T. Nakato, A. Kusuno, T. Kakuchi, *J. Polym. Sci., Part A: Polym. Chem.* **2000**, *38*, 117.
[39] M. Tomida, T. Nakato, S. Matsunami, T. Kakuchi, *Polymer* **1997**, *38*, 4733.
[40] C. Cha, J. H. Jeong, X. Tang, A. T. Zill, Y. S. Prakash, S. C. Zimmerman, T. A. Saif, H. Kong, *Bioconjug. Chem.* **2011**, *22*, 2377.
[41] J. Hong, J. Han, C. Cha, *Int. J. Mol. Sci.* **2022**, *23*, 5044.
[42] S. Kim, C. Choi, C. Cha, *Adv. Healthcare Mater.* **2021**, *10*, 2101109.
[43] J. Hong, Y. Shin, J. Lee, C. Cha, *Lab Chip* **2021**, *21*, 710.
[44] J.-H. Lee, T.-H. Lee, K.-S. Shim, J.-W. Park, H.-J. Kim, Y. Kim, S. Jung, *Int. J. Adhes. Adhes.* **2017**, *74*, 137.